

Analyzing Adversarial Robustness of Vision Transformers against Spatial and Spectral Attacks

Gihyun Kim and Jong-Seok Lee
Yonsei University, Republic of Korea
{khh9314,jong-seok.lee}@yonsei.ac.kr

Abstract—Vision Transformers have emerged as a powerful architecture that can outperform convolutional neural networks (CNNs) in image classification tasks. Several attempts have been made to understand robustness of Transformers against adversarial attacks, but existing studies draw inconsistent results, i.e., some conclude that Transformers are more robust than CNNs, while some others find that they have similar degrees of robustness. In this paper, we address two issues unexplored in the existing studies examining adversarial robustness of Transformers. First, we argue that the image quality should be simultaneously considered in evaluating adversarial robustness. We find that the superiority of one architecture to another in terms of robustness can change depending on the attack strength expressed by the quality of the attacked images. Second, by noting that Transformers and CNNs rely on different types of information in images, we formulate an attack framework, called Fourier attack, as a tool for implementing flexible attacks, where an image can be attacked in the spectral domain as well as in the spatial domain. This attack perturbs the magnitude and phase information of particular frequency components selectively. Through extensive experiments, we find that Transformers tend to rely more on phase information and low frequency information than CNNs, and thus sometimes they are even more vulnerable under frequency-selective attacks. It is our hope that this work provides new perspectives in understanding the properties and adversarial robustness of Transformers.



1 INTRODUCTION

CONVOLUTION neural networks (CNNs) have been a dominant neural network architecture in computer vision for a long time. However, Transformer-based structures have recently emerged as another promising architecture [1], achieving even better performance than CNNs especially in image classification.

CNNs are known to be vulnerable to adversarial attacks, i.e., an imperceptible perturbation added to an image can fool a trained CNN so that it misclassifies the attacked image [2]. Investigating robustness of a model against adversarial attacks is important because not only the vulnerability issue is critical in security-sensitive applications but also such investigation can lead to better understanding of the operating mechanism of the model. Then, a naturally arising question is: how vulnerable are Transformers compared to CNNs?

The researches comparing adversarial robustness of CNNs and Transformers do not reach consistent conclusions. One group of studies claims that Transformers are more robust to adversarial attacks than CNNs [3], [4], [5], [6]. However, another group of studies claims that the two architectures have similar levels of robustness [7], [8], [9].

As an effort to further investigate the adversarial robustness of Transformers, we address two issues that have been unexplored previously. First, we argue that the visual quality of the attacked images needs to be considered properly when adversarial robustness is evaluated. We note that the existing studies often consider only a limited number of conditions regarding the amount of adversarial perturbation (i.e., attack strength). However, the superiority in terms of robustness between models may change depending on the

amount of perturbation. In addition, different attack methods control the amount of perturbation with different algorithmic parameters (e.g., L_∞ norm), which makes it difficult to compare their results. Moreover, the perturbations optimized for different models by different attack methods may have different visual patterns, for which algorithmic parameters may be inadequate to be a criterion of the amount of perturbation. Therefore, we suggest using image quality to represent the amount of perturbation, and also considering a wide range of image quality for comprehensive analysis. Second, noting that different models rely on different features in images, we consider a flexible attack framework to effectively attack both CNNs and Transformers. Previous studies identify that Transformers tend to rely more on low frequency features [4], [10], while CNNs focus more on high frequency features [11], [12]. Popular gradient-based attack methods tend to perturb high frequency features in images, which may make CNNs be fooled more easily than Transformers. We formulate an attack framework, called *Fourier attack*, which can perturb images flexibly in both spatial and spectral domains.

Considering these issues, we conduct extensive experiments to compare adversarial robustness of popular off-the-shelf CNN and Transformer models. Our contributions can be summarized as follows.

- We evaluate various models of CNN and Transformer over a wide range of image quality of attacked images because the relative robustness between models sometimes changes depending on the

image quality.

- We formulate the Fourier attack framework that can perturb the magnitude and phase spectra in the spectral domain and the pixel values in the spatial domain. In particular, examining frequency-selective perturbations by the attacks is the key to deeper understandings of the adversarial robustness of Transformers.
- We conduct in-depth analyses to investigate the frequency-dependent behaviours and importance of spectral information in Transformers.

2 RELATED WORKS

2.1 Vision Transformers

The vision Transformer (ViT) has appeared as a powerful neural architecture using the self-attention mechanism [1]. Several variants of ViT have been also proposed. The Swin Transformer [13] improves the efficiency over ViT using a shifted window scheme for self-attention. To resolve the issue that Transformers require a large dataset for training, the data-efficient image Transformer (DeiT) [14] is trained through distillation from a CNN teacher. Other variants include token-to-token ViT [15], pyramid ViT [16], Transformer in Transformer [17], cross-covariance image Transformer [18], etc.

2.2 Adversarial Attack Methods

The goal of a typical adversarial attack is to change the classification result of a model by injecting a noise-like perturbation to the image while the perturbation is kept imperceptible in order not to be detected easily. The perturbation is usually found via gradient-based optimization. The fast gradient sign method (FGSM) [19] uses the sign of gradient of the classification loss. The projected gradient descent (PGD) method [20] implements a stronger attack by iteratively optimizing the perturbation. These attacks limit the L_p norm of the perturbation to control the imperceptibility. The C&W attack [21] optimizes the weighted sum of the amount of perturbation and the classification loss, which is known to be one of the strongest attacks. Frequency-domain filtering can be used to constrain perturbations only in certain frequency regions [22], [23], [24], which are still based on image-domain attacks. On the other hand, we directly perturb the magnitude and phase spectra. Note that we do not intend to develop a new stronger attack in the frequency domain, but aim to formulate a unified attack framework that can perturb the pixel values, magnitude spectrum, and phase spectrum of an image separately or simultaneously in a flexible manner.

2.3 Adversarial Robustness of Transformers

As mentioned in the introduction, two conflicting conclusions exist in the literature regarding the relative adversarial robustness of CNNs and Transformers. In one group of studies, it is claimed that Transformers are more robust than CNNs. [4], [5], [6], [25] commonly make a conclusion that Transformers are more robust against gradient-based attacks including FGSM, PGD, and C&W because CNNs rely on high frequency information while Transformers do

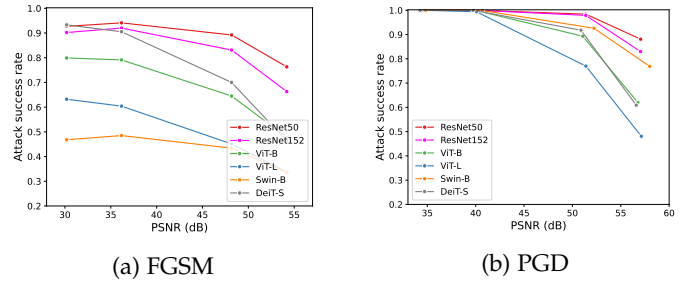


Fig. 1: PSNR vs. attack success rate for CNNs and Transformers under the FGSM and PGD attacks.

not. In addition, [4] claim that the shift-invariant property of CNNs might be a reason for their lower robustness. Another group of studies argues that Transformers are as vulnerable to attacks as CNNs. [8] find that ViTs are not advantageous over the ResNet and big transfer (BiT) models [26] in terms of robustness against various attack methods such as FGSM, PGD, and C&W. [9] show that CNNs and Transformers are similarly vulnerable against various natural and adversarial perturbations. [7] attempt to compare CNNs and Transformers on a common training setup, from which it is concluded that they have similar adversarial robustness.

The aforementioned studies usually do not consider the trade-off characteristics between vulnerability and attack strength in an extensive manner over a wide range of image quality degradation. In addition, most of the studies consider only pixel-domain perturbations. These issues are dealt with in our work.

3 METHOD

In this section, we present the two issues considered in our comparison of adversarial robustness of CNNs and Transformers, and explain how we perform the comparison.

3.1 Consideration of Image Quality

In many popular attack methods, the attack strength can be controlled by certain parameters (e.g., L_∞ norm of perturbation in FGSM, the balancing parameter between the amount of distortion and the change of the classification loss in C&W). As an attack becomes strong, the target model becomes more vulnerable, but the image distortion may become perceptible. In the previous studies, such a trade-off relationship has not been fully considered in benchmarking the adversarial robustness of Transformers. However, depending on the considered attack strength, the superiority of one model to another in terms of robustness may vary. Fig. 1 shows an example of this issue, which shows the attack success rate (ASR) on CNNs and Transformers with respect to the attack strength (represented as the image quality in peak signal-to-noise ratio (PSNR)) for the FGSM and PGD attacks (see the Appendix for the experimental setup). Overall, the ResNet models tend to be more vulnerable than the Transformers in both attacks by showing higher ASR, which is consistent with the results in [4], [5], [6]. When we have a look at the details, additional observations can be also made. For instance, in Fig. 1a, DeiT-S is more robust than both ResNet models over 40 dB but they show

similar vulnerability at 30-35 dB. In addition, in Fig. 1b, all models are similarly vulnerable showing almost 100% of ASR for low PSNR values, but their vulnerability becomes different after about 40 dB. These results demonstrate that it is important to examine a wide range of image quality in order to better understand the vulnerability of different models.

While the attack strength and image quality are generally compatible in the context of adversarial attack, we consider the latter as a more proper way due to the following reasons. (1) The attack strength does not consider visual perception of the perturbation unlike image quality. PSNR is defined in the signal point of view but already shows moderately high correlation with human perception [27], and thus has potential as an image quality metric for robustness evaluation. Furthermore, many perceptual image quality metrics have been developed in literature, which can be used to measure the perceptual amount of perturbation. (2) At the same attack strength, the perturbations optimized by different attack methods on different models may have visually different patterns, which need to be quantified appropriately. As a hypothetical example of an L_∞ norm-constrained attack, consider that a perturbation has a nonzero value at a single pixel location, while another perturbation has nonzero values at many pixel locations over the whole image. Both cases satisfy the constraint, but they should be treated differently, which can be accomplished using an image quality metric. (3) As aforementioned, different attack methods use different algorithmic parameters to control the attack strength, which cannot be easily compared with each other. This problem is readily resolved if an image quality metric is used. (4) We consider an attack framework perturbing different components (i.e., magnitude, phase, and pixel). It is observed that the perturbation patterns are significantly different depending on the target component. An image quality metric is required in order to compare the attack strengths in different components properly.

3.2 Fourier Attack

Different from the existing works, we formulate a unified attack framework, called Fourier attack, to attack images both spatially and spectrally. The following considerations motivate us to use the framework. First, the previous studies point out that CNNs tend to rely on high frequency information in images, which is why they appear more vulnerable than Transformers [4], [5]. In other words, the popular attack methods injecting high frequency noise are disadvantageous to CNNs. Our attack framework tries to alleviate such an inherent bias by enabling to flexibly perturb images in both spatial location-selective and frequency-selective manners. Second, we aim to analyze the mechanisms of Transformers in various viewpoints through the results of attacks in different domains.

The Fourier transform of an image X can be written by

$$\mathcal{F}\{X\} = M \cdot e^{j\phi}, \quad (1)$$

where M and ϕ are the magnitude and phase spectra, respectively. The image is attacked by the combination

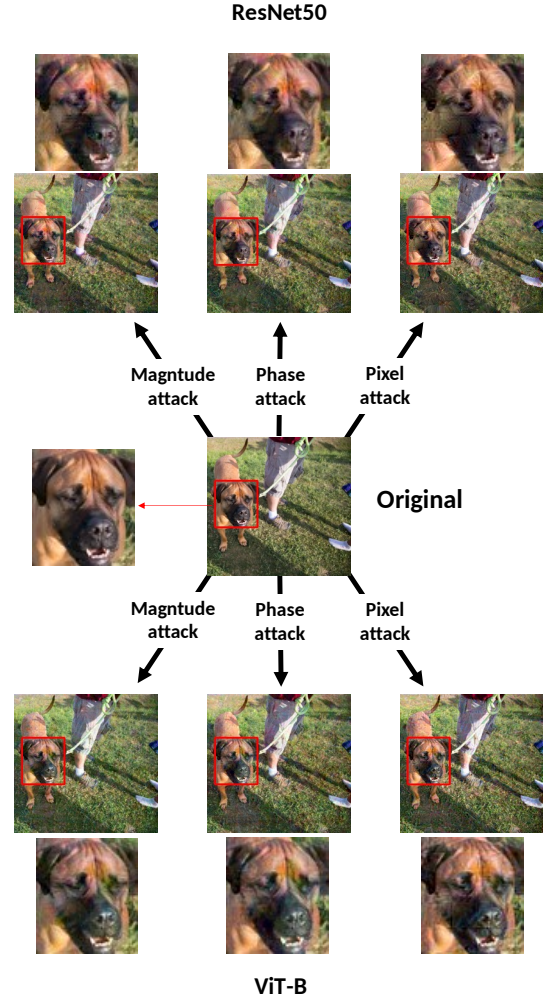


Fig. 2: Example case of our attack perturbing the magnitude, phase, and pixel values, respectively, for ResNet50 and ViT-B.

of multiplicative magnitude perturbation¹ δ_{mag} , additive phase perturbation δ_{phase} , and additive pixel perturbation δ_{pixel} as follows:

$$\tilde{X}' = \mathcal{F}^{-1} \left\{ \text{clip}_{0,\infty}(M \otimes \delta_{\text{mag}}) \cdot e^{j(\phi + \delta_{\text{phase}})} \right\} + \delta_{\text{pixel}}, \quad (2)$$

$$X' = \text{clip}_{0,1}(\tilde{X}'), \quad (3)$$

where \mathcal{F}^{-1} is the inverse Fourier transform, \otimes is the element-wise multiplication, and $\text{clip}_{a,b}(x)$ clips each element of x within a and b . Here, we assume that the pixel values are normalized within 0 and 1. Note that δ_{mag} and δ_{phase} are kept to be symmetric in order to ensure the resulting image after the inverse Fourier transform to have real-valued pixel values.

We consider various combinations of employed perturbations, i.e., single component attacks employing only one among δ_{mag} , δ_{phase} , and δ_{pixel} , denoted as “magnitude attack,” “phase attack,” and “pixel attack,” respectively,

1. We also tried an additive magnitude perturbation but it was not optimized well because the magnitude spectrum has values over a wide range.

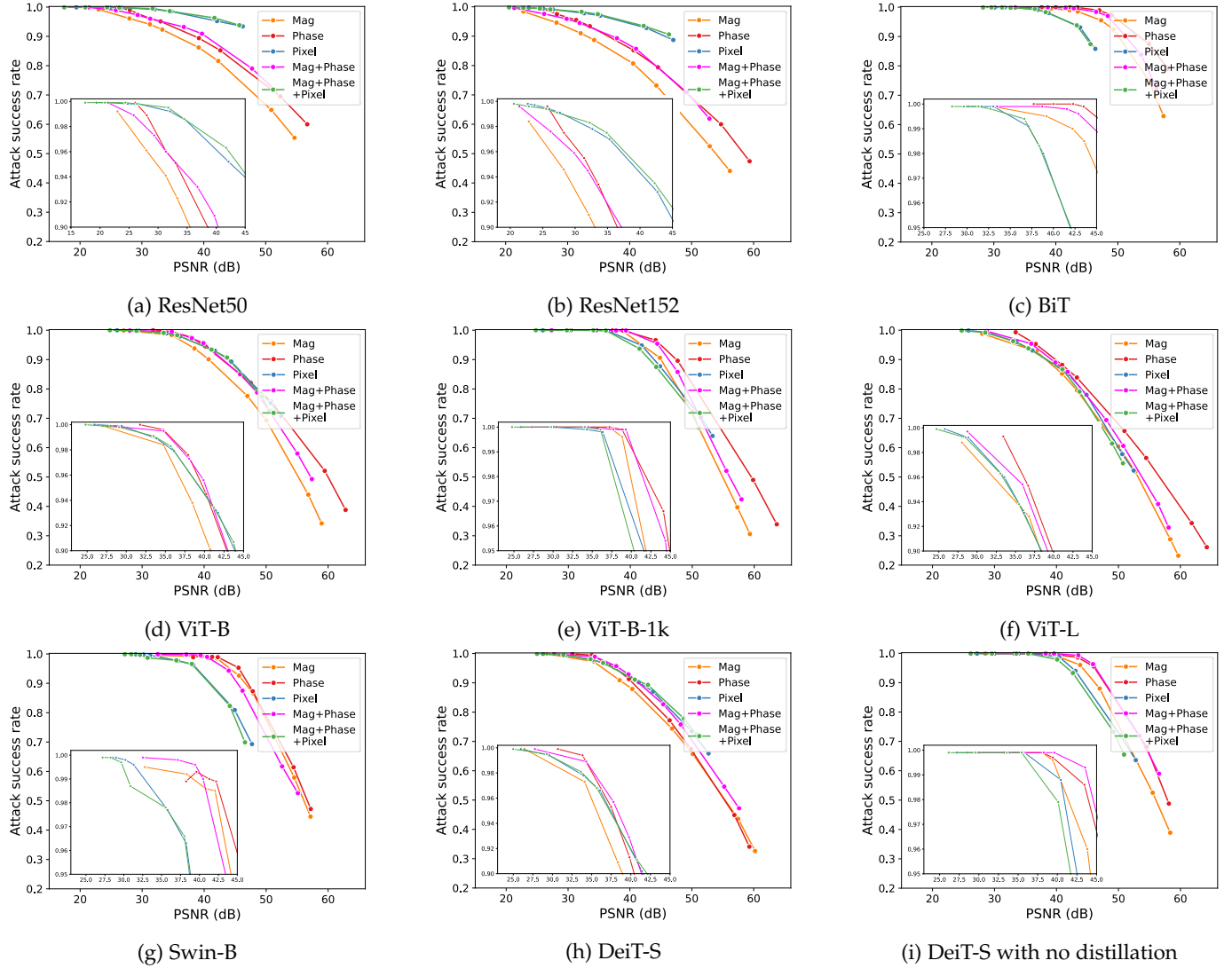


Fig. 3: Comparison of different attacks for each model. The range for high attack success rates is enlarged for better visualization.

the attack employing both δ_{mag} and δ_{phase} , denoted as “mag+phase attack,” and the attack employing all perturbations, denoted as “mag+phase+pixel attack.”

The process to optimize the perturbations is inspired by the C&W attack [21]. In other words, we minimize the L_2 difference (i.e., mean squared error (MSE)) between the original and attacked images and maximize the cross-entropy (CE) loss. Thus, the loss function of our attack is given by

$$\text{Loss} = \lambda \cdot \text{MSE}(X', X) - \text{CE}(f(X'), y), \quad (4)$$

where λ is a parameter balancing MSE and CE, $f(\cdot)$ is the model, and y is the ground truth class label.

Fig. 2 shows an example case, where each of the magnitude, phase, and pixel components is perturbed. It can be observed that attacking different components induce different distortion patterns in the image. The distortion pattern also varies depending on the target model.

4 EXPERIMENTS

4.1 Setup

We aim to benchmark the adversarial robustness of the pre-trained models that serve as off-the-shelf solutions in general image classification applications. We consider ResNet50, ResNet152, and BiT as CNNs, and ViT-B/16, ViT-L/16, DeiT-S, and Swin-B as Transformers. Here, S, B and L mean small, base, and large, and /16 means the patch size. ResNet50 and ResNet152 are from the torchvision models [28] trained on ImageNet-1k [29]. BiT based on ResNet152x4, ViT-B, ViT-L, DeiT-S, and Swin-B are from the timm module [30], which are pretrained on ImageNet-21k [31] and finetuned on ImageNet-1k. ViT trained on ImageNet-1k and DeiT-S without distillation are also considered.

To evaluate adversarial robustness of the models, the image dataset from the NeurIPS 2017 Adversarial Challenge [32] is used. For BiT, the images are resized to 480×480 to match the input dimension.

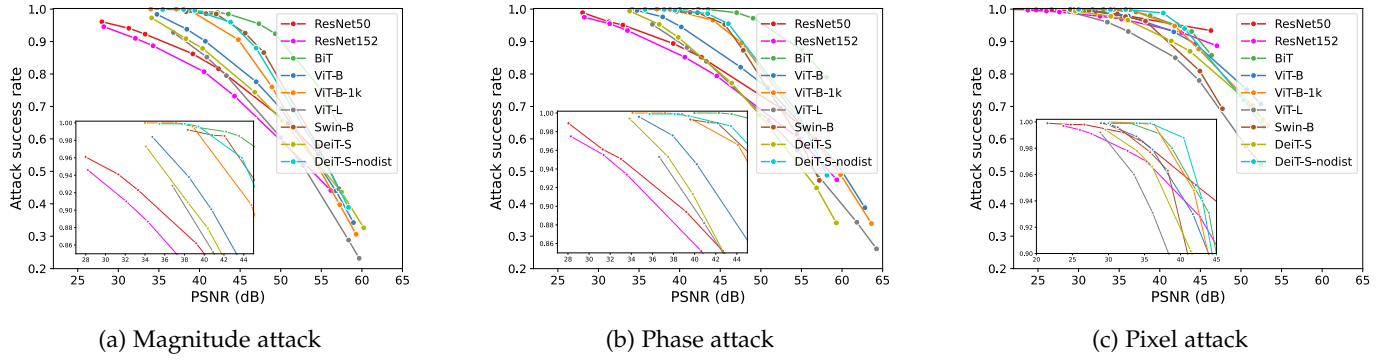


Fig. 4: Comparison of different models for each attack type. The range for high attack success rates is enlarged for better visualization.

To optimize the perturbations, we use the Adam optimizer with a fixed learning rate of 5×10^{-3} and a weight decay parameter of 5×10^{-6} . The maximum number of iterations is set to 1000. We also set a termination condition that the optimization stops when the loss in Eq. (4) does not improve for five consecutive iterations. We vary the value of λ as $\{1, 10^3, 5 \times 10^3, 10^4, 5 \times 10^4, 10^5, 5 \times 10^5, 10^6\}$.

We report the results using PSNR as the image quality metric. The results using other metrics, mean deviation similarity index (MDSI) [33] and learned perceptual image patch similarity (LPIPS) [34], are shown in the Appendix.

4.2 Results

4.2.1 Comparison of Attacks

We first compare different attacks in our attack framework in order to show the effectiveness of attacking in the spectral domain. Fig. 3 shows the results in terms of ASR with respect to PSNR. All the attacks can achieve (almost) 100% of ASR at the lower extremes of PSNR for all models. However, their relative effectiveness varies depending on the model. For ResNet50 and ResNet152, the pixel attack appears stronger than the magnitude attack and the phase attack, whereas the phase attack is the strongest for ViTs and Swin-B. This shows that the flexible frequency domain attack overcomes the limitation of the pixel attack perturbing mainly high frequency information, and becomes a strong attack on the Transformers. DeiT-S is more vulnerable to the pixel attack as in the ResNet models, probably because it is trained using distillation from the CNN teacher, which is supported by the observation that DeiT-S without distillation is more vulnerable to the phase attack as in ViTs and Swin-B. It is observed that the mag+phase attack tends to be similar to or weaker than the single component attacks for ResNets or Transformers, respectively; it seems that using more variables to be optimized makes optimization more challenging. And, perturbing all components (i.e., the magnitude+phase+pixel attack) does not improve the attack performance compared to the pixel attack for all models. Thus, we consider only the single component attacks in the following analyses. Another observation is that the phase attack is mostly stronger than the magnitude attack. Further analysis on this is presented later.

4.2.2 Comparison of Vulnerability of Models.

Fig. 4 compares ASR of the models with respect to PSNR for each attack type. Most importantly, when ASR is relatively high, the Transformers are similar to or more robust than the ResNet models under the pixel attack (as in the case of PGD in Fig. 1b) but more vulnerable to the magnitude and phase attacks. Again, this is due to the flexible perturbations in the frequency domain, which will be further analyzed later. When PSNR is high (over 45-50 dB), these trends do not hold any more, i.e., some Transformers (ViTs and DeiT-S) become similarly robust to the ResNet models under the magnitude and phase attacks, and the ResNet models become more vulnerable to all Transformers under the pixel attack. When Swin-B is compared to ViT-B and ViT-L, the former shows higher vulnerability than the latter for the magnitude and phase attacks. When the model size is concerned, larger models (ViT-L and ResNet152) are more robust than smaller models (ViT-B and ResNet50) under all attacks. While [9] also observed a similar trend using pixel-domain attacks (FGSM and PGD), we find that the same also holds for the attacks in the spectral domain. When ViT-B and ViT-B-1k are compared, ViT-B is more robust than ViT-B-1k, but becomes more vulnerable when PSNR becomes high, especially for the pixel attack. [9] noted that training with a larger dataset is beneficial for robustness; we additionally find that the benefit of a larger dataset is even more prominent for the magnitude and phase attacks than for the pixel attack, but the benefit disappears when the amount of perturbation is small. DeiT-S behaves more like ResNet than the other Transformers due to the distillation using CNN. It is interesting to see that BiT, which has the ResNet structure, shows the highest vulnerability to the magnitude and phase attacks and is one of the most vulnerable models under the pixel attack. [8] experimented the C&W attack, which can be considered to be similar to our pixel attack, but all models recorded 100% of ASR and thus no comparative conclusion could be made; in contrast, our result considering a wide range of image quality for the pixel attack reveals the high vulnerability of BiT.

4.3 Analysis

We further investigate the particular vulnerability of the Transformers to the attacks in the spectral domain.

4.3.1 Frequency Analysis of Perturbations.

We examine the distortion due to the attack in the spectral viewpoint. For this, the Fourier transform is applied to the difference between the attacked image and the original image, and the magnitudes in different frequency regions are obtained, where the frequency regions are defined as shown in Fig. 5b. Figs. 5c to 5g show the attacked image, distortion in the pixel domain, and magnitude distribution under the phase attack. The averaged results over images are shown in the Appendix. In the case of ResNet50, the distortion is concentrated on the high frequency regions, whereas low frequency regions are mainly distorted in the other models. Since CNNs and Transformers rely more on high and low frequency information, respectively [4], [10], [11], [12], the attack effectively injects perturbations in such vulnerable frequency regions. Consequently, the distortion pattern significantly differs according to those properties. Unlike ResNet50, the distortion in BiT is extremely concentrated in the low frequency regions, which explains why BiT is the most vulnerable under the phase attack in Fig. 4b.

4.3.2 Frequency-Restricted Attacks.

We examine the case where the perturbation is applied to only a limited frequency band. Fig. 6 compares the phase attack when the phase perturbation is only in the low frequency band (regions 1 and 2 in Fig. 5b) or the high frequency band (region 10 in Fig. 5b). For ResNet50, it is more effective to perturb only the high frequency band because high frequency perturbations for which ResNet50 becomes particularly vulnerable can be optimized more easily by the restriction. However, for ViT-B, perturbing only the high frequency band is the least effective and the case without restriction implements the strongest attack, because low-intermediate frequency regions need to be perturbed for an effective attack as shown in Fig. 5e.

4.4 Dependence on Magnitude and Phase

In most results above, the magnitude attack appears to be weaker than the phase attack. We investigate this phenomenon further.

4.4.1 Sensitivity to Reduced Magnitude and Phase.

We design an experiment where the magnitude or phase spectrum is reduced gradually, i.e., $M' = M \times (1 - r)$ or $\phi' = \phi \times (1 - r)$, where $r \in \{0, 0.1, \dots, 0.9, 1\}$, and the classification accuracy is measured. Note that no attack is applied in this experiment. The results are shown in Fig. 7. Both ResNet50 and ViT-B are more sensitive to phase reduction than magnitude reduction, and in particular, ViT-B achieves 85.6% of accuracy even though the magnitude is reduced by 90%. These imply that the corruption of the magnitude spectrum is less critical than that of the phase spectrum, which explains the severer vulnerability of the models to the phase attack.

4.4.2 Magnitude-Phase Recombination.

Inspired by [35], we conduct an experiment where the magnitude component of one image and the phase component of another image are recombined in the frequency domain and the classification result of this recombined image (after

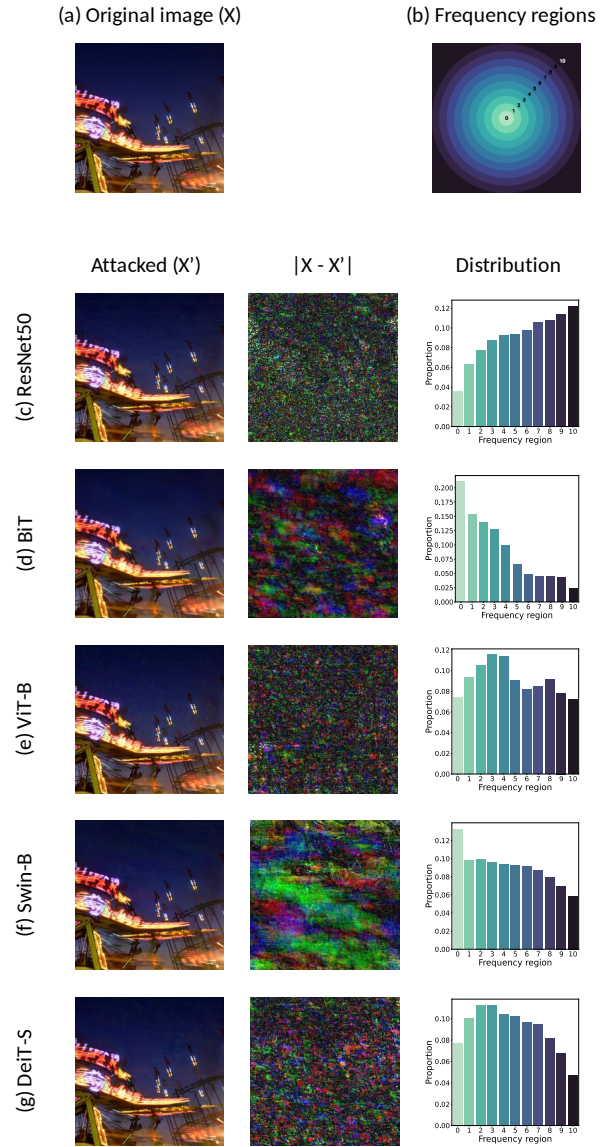


Fig. 5: Example of the attacked image, distortion in the pixel domain (magnified by $\times 20$), and distribution of the distortion over different frequency regions.

inverse Fourier transform) from a model is tested. For all possible image pairs, TABLE 1 shows the proportion of the images that are classified as the class of the magnitude image or phase image, or none of the two classes. For ResNet50, most of the cases (97.85%) do not follow either the classes of the magnitude or the phase, while for the rest, more images follow the phase classes (2.04%) than the magnitude classes (0.11%). For ViT-B, however, a considerable amount of recombined images (33.92%) are classified as the class of the phase images, while only 0.26% of the images follow the classes of the magnitude images. These results highlight the relative importance of the phase information, providing an explanation on the particular vulnerability of the Transformers to the phase attack and the higher strength of the phase attack than the magnitude attack for the Transformers.

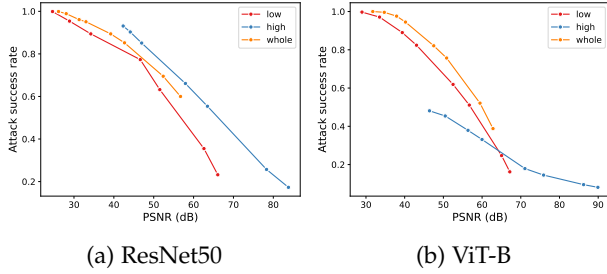


Fig. 6: Results of the phase attack when the perturbation is restricted to reside only in the low or high frequency band. The case without restriction is also shown as ‘whole.’

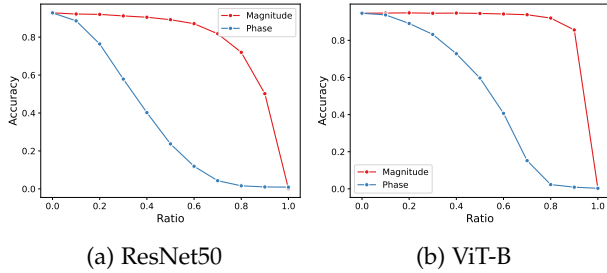


Fig. 7: Classification accuracy with respect to the ratio of reduction in the magnitude or phase spectrum.

Model	Phase (%)	Magnitude (%)	Else (%)
ResNet50	2.04	0.11	97.85
ViT-B	33.92	0.26	65.82

TABLE 1: Proportions of magnitude-phase-recombined images that are classified to the classes of the magnitude or phase images, or some other classes.

5 CONCLUSION

We comparatively investigated adversarial robustness of CNNs and Transformers using the Fourier attack framework with consideration of the relationship between the image quality and ASR. Our major findings can be summarized as follows.

- Different from the conclusions of the existing studies, we observed that Transformers can become more vulnerable than CNNs. The Transformers are more robust than the ResNets under the pixel attack, but more vulnerable under the magnitude and phase attacks. However, when the attack strength is low and the image quality becomes high, the ResNets tend to become more vulnerable than the Transformers.
- Some models including DeiT and BiT sometimes do not follow the above trend. DeiT trained by distillation from CNN behaves more similarly to ResNets. BiT appears to be more vulnerable than the other models even under the magnitude and phase attacks.
- The ResNets are sensitive to the perturbation in high frequency regions, which can be effectively injected by the pixel attack. On the other hand, the Transformers are sensitive to the perturbation in low frequency regions, which can be optimized in the frequency domain by the phase attack.

- The phase information plays more important role in classification for both ResNets and Transformers than the magnitude information, and reliance on the phase information is more prominent in Transformers.

APPENDIX A EXPERIMENTAL ENVIRONMENTS

We run our experiments on an NVIDIA GeForce RTX 3090 GPU using CUDA 11.2. The software modules are listed in the following table.

Module	Version
torch	1.11.0
torchvision	1.12.0
opencv-python	4.5.4.60
timm	0.5.4
piq	0.7.0
numpy	1.21.2
Pillow	8.4.0
seaborn	0.11.2
pandas	1.3.5

APPENDIX B EXPERIMENTAL SETUP FOR FGSM AND PGD

The amount of perturbation is limited by the L_∞ norm $\epsilon \in \{0.1/255, 0.5/255, 1/255, 4/255, 8/255\}$ for both FGSM and PGD. For PGD, the step size at each iteration is set to ϵ/T , where T is the number of iterations ($T = 50$).

APPENDIX C RESULTS USING OTHER IMAGE QUALITY METRICS

While we use PSNR as the image quality metric in the main paper, results using other perceptual image quality metrics are shown here. We choose the mean deviation similarity index (MDSI) [33], which was shown to perform the best in [36], and learned perceptual image patch similarity (LPIPS) [34], which uses the features from a pre-trained network for classification. The results are shown in Figs. 8-11. Note that a larger value of MDSI or LPIPS indicates a lower quality level. Overall, the trends remain similar to those shown in Figs. 3 and 4.

APPENDIX D AVERAGE DISTRIBUTION OF DISTORTION

The distributions of the distortion by the phase attack over different frequency regions, averaged over all images, are shown in Fig. 12. The trends are the same to those observed in Fig. 5.

REFERENCES

- [1] A. Dosovitskiy, L. Beyer, A. Kolesnikov, D. Weissenborn, X. Zhai, T. Unterthiner, M. Dehghani, M. Minderer, G. Heigold, S. Gelly *et al.*, “An image is worth 16x16 words: Transformers for image recognition at scale,” in *Proceedings of the 9th International Conference on Learning Representations*, 2021.
- [2] N. Akhtar and A. Mian, “Threat of adversarial attacks on deep learning in computer vision: A survey,” *IEEE Access*, vol. 6, pp. 14410–14430, 2018.

- [3] M. M. Naseer, K. Ranasinghe, S. H. Khan, M. Hayat, F. Shahbaz Khan, and M.-H. Yang, "Intriguing properties of vision transformers," in *Advances in Neural Information Processing Systems*, vol. 34, 2021, pp. 23 296–23 308.
- [4] P. Benz, S. Ham, C. Zhang, A. Karjauv, and I. S. Kweon, "Adversarial robustness comparison of vision transformer and mlp-mixer to cnns," in *Proceedings of the 32nd British Machine Vision Conference*, 2021.
- [5] R. Shao, Z. Shi, J. Yi, P.-Y. Chen, and C.-J. Hsieh, "On the adversarial robustness of vision transformers," 2021.
- [6] A. Aldahdooh, W. Hamidouche, and O. Deforges, "Reveal of vision transformers robustness against adversarial attacks," 2021.
- [7] Y. Bai, J. Mei, A. L. Yuille, and C. Xie, "Are transformers more robust than cnns?" in *Advances in Neural Information Processing Systems*, vol. 34, 2021, pp. 26 831–26 843.
- [8] K. Mahmood, R. Mahmood, and M. Van Dijk, "On the robustness of vision transformers to adversarial examples," in *Proceedings of the IEEE/CVF International Conference on Computer Vision*, 2021, pp. 7838–7847.
- [9] S. Bhojanapalli, A. Chakrabarti, D. Glasner, D. Li, T. Unterthiner, and A. Veit, "Understanding robustness of transformers for image classification," in *Proceedings of the IEEE/CVF International Conference on Computer Vision*, 2021, pp. 10 231–10 241.
- [10] N. Park and S. Kim, "How do vision transformers work?" in *Proceedings of the 10th International Conference on Learning Representations*, 2022.
- [11] H. Wang, X. Wu, Z. Huang, and E. P. Xing, "High-frequency component helps explain the generalization of convolutional neural networks," in *Proceedings of the IEEE/CVF Conference on Computer Vision and Pattern Recognition*, 2020, pp. 8684–8694.
- [12] J. Jo and Y. Bengio, "Measuring the tendency of cnns to learn surface statistical regularities," 2017.
- [13] Z. Liu, Y. Lin, Y. Cao, H. Hu, Y. Wei, Z. Zhang, S. Lin, and B. Guo, "Swin transformer: Hierarchical vision transformer using shifted windows," in *Proceedings of the IEEE/CVF International Conference on Computer Vision*, 2021, pp. 10 012–10 022.
- [14] H. Touvron, M. Cord, M. Douze, F. Massa, A. Sablayrolles, and H. Jégou, "Training data-efficient image transformers & distillation through attention," in *Proceedings of the 38th International Conference on Machine Learning*, 2021, pp. 10 347–10 357.
- [15] L. Yuan, Y. Chen, T. Wang, W. Yu, Y. Shi, Z.-H. Jiang, F. E. Tay, J. Feng, and S. Yan, "Tokens-to-token vit: Training vision transformers from scratch on imagenet," in *Proceedings of the IEEE/CVF International Conference on Computer Vision*, 2021, pp. 558–567.
- [16] W. Wang, E. Xie, X. Li, D.-P. Fan, K. Song, D. Liang, T. Lu, P. Luo, and L. Shao, "Pyramid vision transformer: A versatile backbone for dense prediction without convolutions," in *Proceedings of the IEEE/CVF International Conference on Computer Vision*, 2021, pp. 568–578.
- [17] K. Han, A. Xiao, E. Wu, J. Guo, C. Xu, and Y. Wang, "Transformer in transformer," in *Advances in Neural Information Processing Systems*, vol. 34, 2021, pp. 15 908–15 919.
- [18] A. Ali, H. Touvron, M. Caron, P. Bojanowski, M. Douze, A. Joulin, I. Laptev, N. Neverova, G. Synnaeve, J. Verbeek *et al.*, "Xcit: Cross-covariance image transformers," in *Advances in Neural Information Processing Systems*, vol. 34, 2021, pp. 20 014–20 027.
- [19] I. J. Goodfellow, J. Shlens, and C. Szegedy, "Explaining and harnessing adversarial examples," in *Proceedings of the 3rd International Conference on Learning Representations*, 2015.
- [20] A. Madry, A. Makelov, L. Schmidt, D. Tsipras, and A. Vladu, "Towards deep learning models resistant to adversarial attacks," in *Proceedings of the 6th International Conference on Learning Representations*, 2018.
- [21] N. Carlini and D. Wagner, "Towards evaluating the robustness of neural networks," in *Proceedings of the IEEE Symposium on Security and Privacy*, 2017, pp. 39–57.
- [22] X.-C. Li, X.-Y. Zhang, F. Yin, and C.-L. Liu, "F-mixup: Attack cnns from fourier perspective," in *Proceedings of the 25th International Conference on Pattern Recognition*, 2020, pp. 541–548.
- [23] C. Guo, J. S. Frank, and K. Q. Weinberger, "Low frequency adversarial perturbation," in *Proceedings of the Uncertainty in Artificial Intelligence*, 2020, pp. 1127–1137.
- [24] Y. Sharma, G. W. Ding, and M. A. Brubaker, "On the effectiveness of low frequency perturbations," in *Proceedings of the 28th International Joint Conference on Artificial Intelligence*, 2019, pp. 3389–3396.
- [25] S. Paul and P.-Y. Chen, "Vision transformers are robust learners," in *Proceedings of the AAAI Conference on Artificial Intelligence*, vol. 36, 2022, pp. 2071–2081.
- [26] A. Kolesnikov, L. Beyer, X. Zhai, J. Puigcerver, J. Yung, S. Gelly, and N. Houlsby, "Big transfer (bit): General visual representation learning," in *Proceedings of the European Conference on Computer Vision*, 2020, pp. 491–507.
- [27] S. Athar and Z. Wang, "A comprehensive performance evaluation of image quality assessment algorithms," *IEEE Access*, vol. 7, pp. 140 030–140 070, 2019.
- [28] A. Paszke, S. Gross, F. Massa, A. Lerer, J. Bradbury, G. Chanan, T. Killeen, Z. Lin, N. Gimelshein, L. Antiga *et al.*, "Pytorch: An imperative style, high-performance deep learning library," in *Advances in Neural Information Processing Systems*, vol. 32, 2019.
- [29] O. Russakovsky, J. Deng, H. Su, J. Krause, S. Satheesh, S. Ma, Z. Huang, A. Karpathy, A. Khosla, M. Bernstein, A. C. Berg, and L. Fei-Fei, "ImageNet Large Scale Visual Recognition Challenge," *International Journal of Computer Vision*, vol. 115, no. 3, pp. 211–252, 2015.
- [30] R. Wightman, "Pytorch image models," <https://github.com/rwightman/pytorch-image-models>, 2019, accessed: 2019-02-02.
- [31] J. Deng, W. Dong, R. Socher, L.-J. Li, K. Li, and L. Fei-Fei, "Imagenet: A large-scale hierarchical image database," in *Proceedings of the IEEE Conference on Computer Vision and Pattern Recognition*, 2009, pp. 248–255.
- [32] R. Wightman, "Nips 2017 adversarial competition (pytorch)," <https://github.com/rwightman/pytorch-nips2017-adversarial>, 2017, accessed: 2017-07-31.
- [33] H. Z. Nafchi, A. Shahkolaei, R. Hedjam, and M. Cheriet, "Mean deviation similarity index: Efficient and reliable full-reference image quality evaluator," *IEEE Access*, vol. 4, pp. 5579–5590, 2016.
- [34] R. Zhang, P. Isola, A. A. Efros, E. Shechtman, and O. Wang, "The unreasonable effectiveness of deep features as a perceptual metric," in *Proceedings of the IEEE conference on Computer Vision and Pattern Recognition*, 2018, pp. 586–595.
- [35] G. Chen, P. Peng, L. Ma, J. Li, L. Du, and Y. Tian, "Amplitude-phase recombination: Rethinking robustness of convolutional neural networks in frequency domain," in *Proceedings of the IEEE/CVF International Conference on Computer Vision*, 2021, pp. 458–467.
- [36] S. Kastyulin, D. Zakirov, and D. Prokopenko, "PyTorch Image Quality: Metrics and measure for image quality assessment," 2019, open-source software available at <https://github.com/photosynthesis-team/piq>. [Online]. Available: <https://github.com/photosynthesis-team/piq>

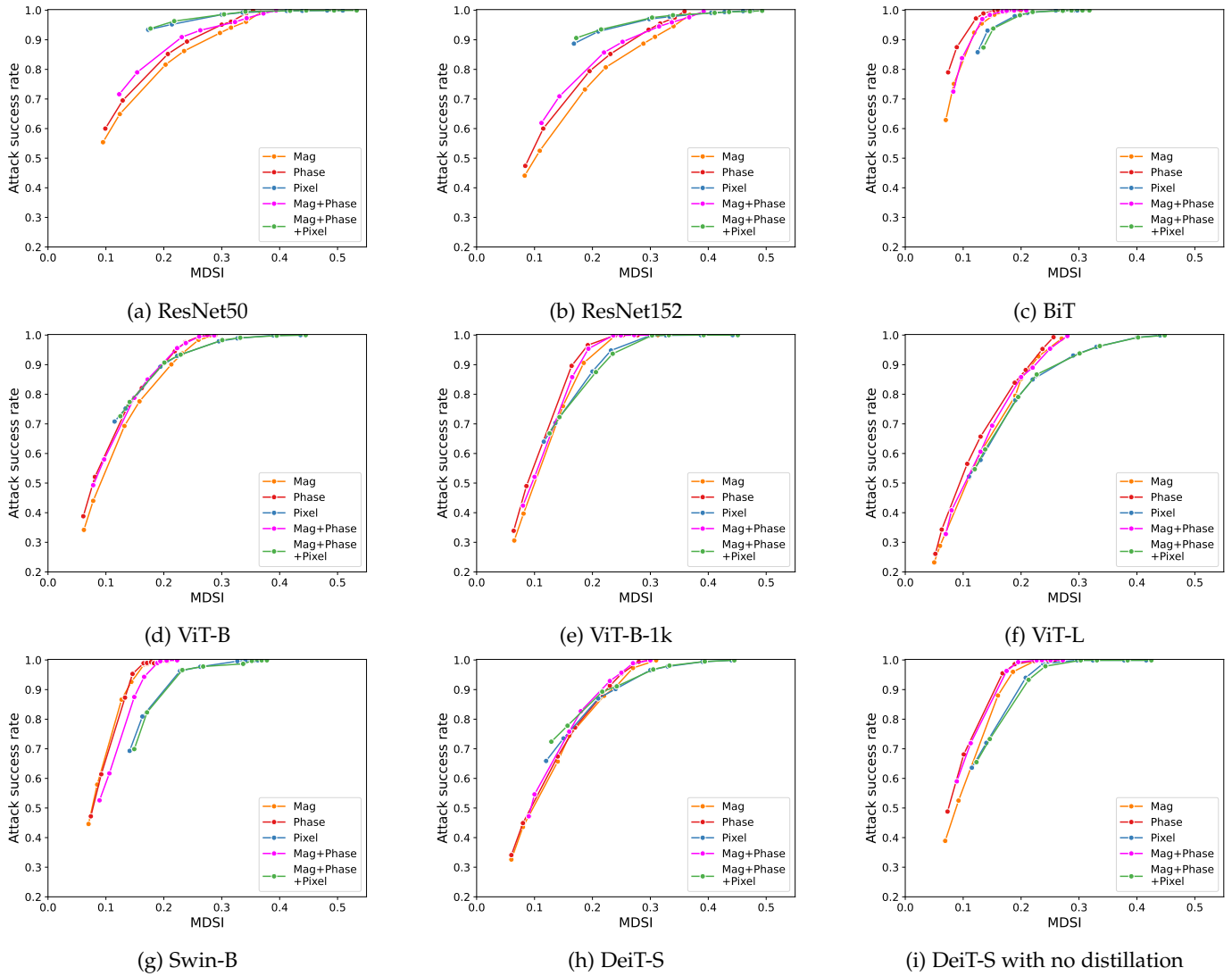


Fig. 8: Comparison of different attacks for each model using MDSI.

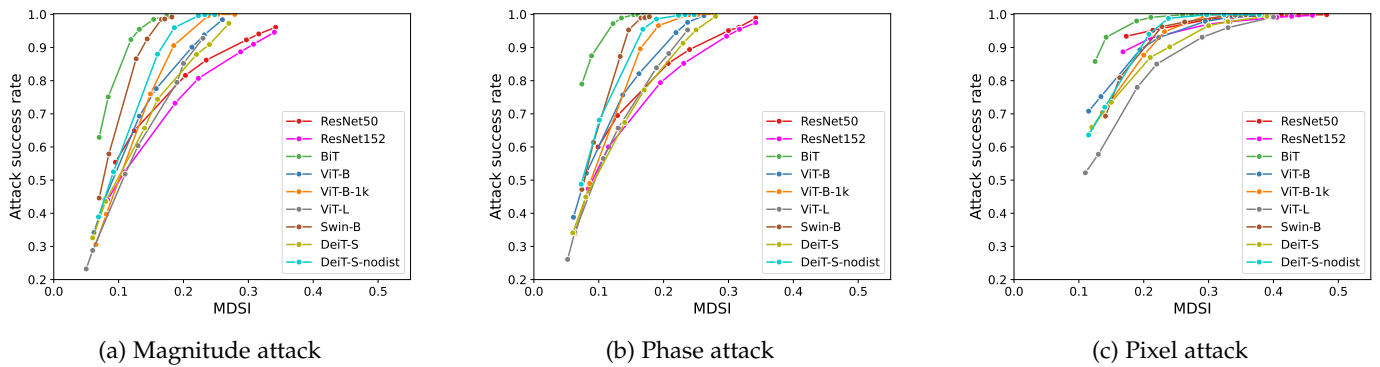


Fig. 9: Comparison of different models for each attack type using MDSI.

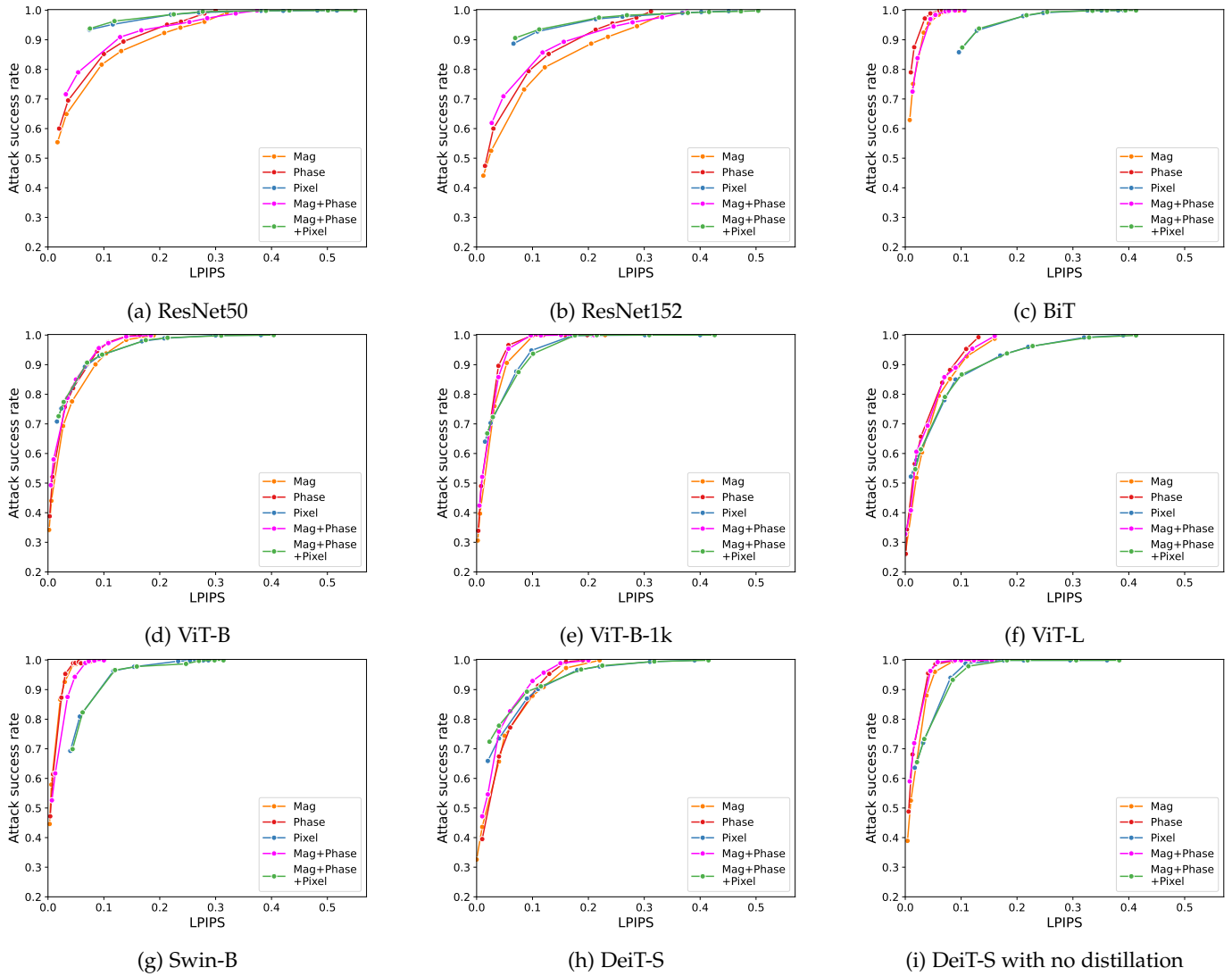


Fig. 10: Comparison of different attacks for each model using LPIPS.

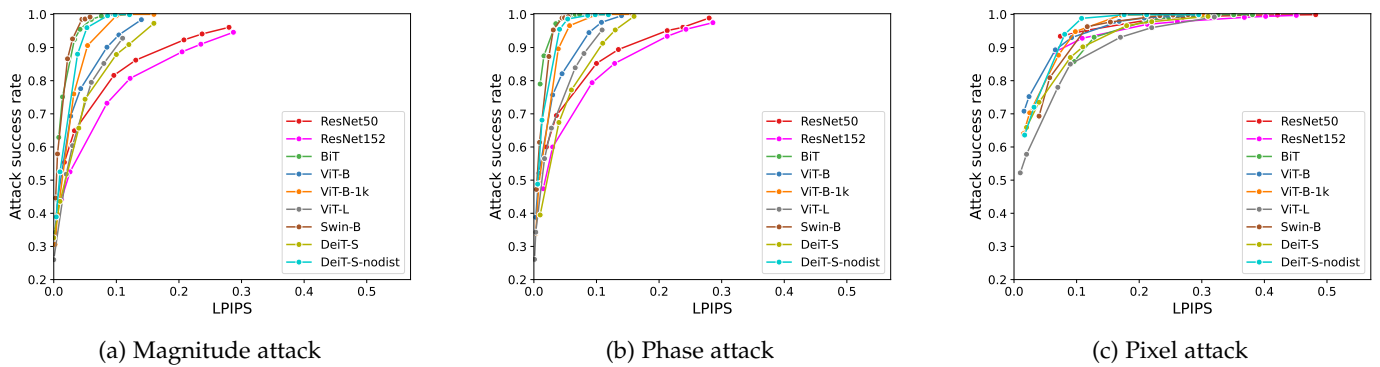


Fig. 11: Comparison of different models for each attack type using LPIPS.

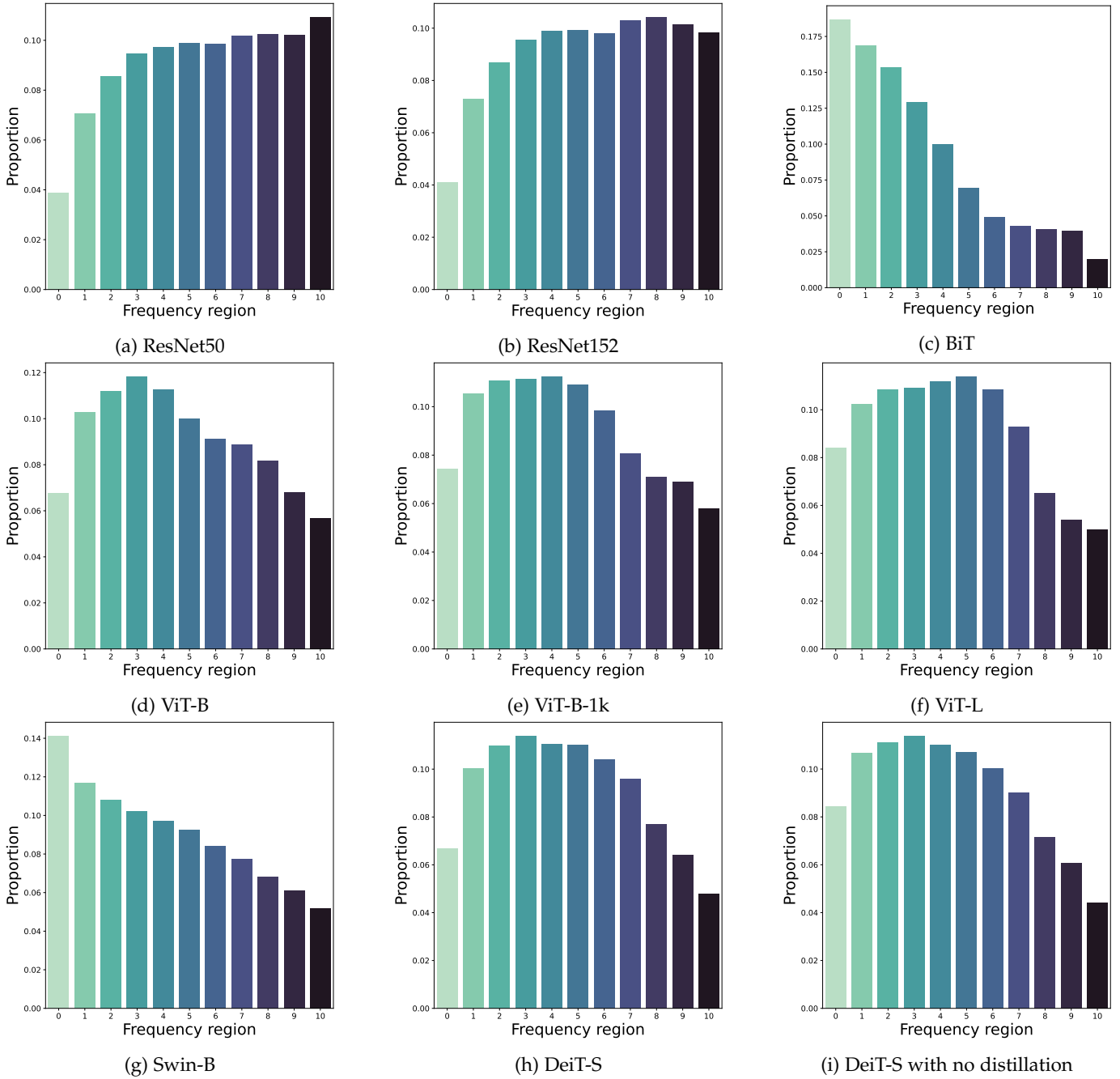


Fig. 12: Average distributions of distortion over different frequency regions.